ChemPubSoc Europe
DOI: 10.1002/cctc.201500966
CHEMCATCHEM
Full Papers

Highly Effective Direct Decomposition of Nitric Oxide by Microwave Catalysis over $BaMeO_3$ (Me = Mn, Co, Fe) Mixed Oxides at Low Temperature under Excess Oxygen

Wentao Xu, Jinjun Cai, Jicheng Zhou,* Yingpiao Ou, Wei Long, Zhimin You, and Yushang Luo[a]

The direct catalytic decomposition of NO with high activity and N_2 selectivity is a great challenge at low temperature under excess oxygen. Herein, we report the NO decomposition by microwave catalysis over $BaMeO_3$ (Me = Mn, Co, Fe) mixed oxides for the first time at low temperature under excess oxygen, for which the $BaCoO_3$ catalyst has an outstanding activity with a high NO conversion and N_2 selectivity up to 99.8% and 99.9%, respectively, even at 250 °C. Comparatively, the best NO conversion is 93.7% for $BaMnO_3$ and only 64.1% for $BaFeO_3$ under microwave irradiation. H_2 temperature-programmed reduction, O_2 temperature-programmed desorption, and the microwave-absorbing properties of the mixed oxides were characterized to illustrate possible reasons that cause such clear differences in the catalytic performance. Importantly, the apparent activation energies for $BaMnO_3$, $BaCoO_3$, and $BaFeO_3$ are as low as 33.4, 13.7, and 46.7 kJ mol^{-1}, respectively, which suggests a significant microwave catalytic effect.

Introduction

Nitrogen oxides (NO_x), emitted from various fixed and mobile sources, are considered as one of the most hazardous pollutants because of their drastic consequences on ecosystems, the atmosphere, and human health.[1,2] The direct decomposition of NO into N_2 and O_2 offers the most attractive and ideal route to remove NO with respect to economic and environmental considerations as the products of the reaction are environmentally friendly and it does not involve the addition of toxic reducing agents, such as NH_3.[3,4] Several catalysts have been investigated for the direct decomposition of NO in the conventional reaction mode (CRM), which include noble metals,[5–7] metal oxides,[8–12] and metal-ion-exchanged zeolites.[13–16] Unfortunately, Cu-ZSM-5 (one of the most active catalysts for the direct decomposition of NO) has a low hydrothermal stability and will be deactivated at temperatures higher than 600 °C, and noble-metal catalysts are expensive and inhibited strongly by oxygen.[17,18] Therefore, composite mixed oxides, which include perovskite-type oxides, are recognized as promising candidates for direct NO decomposition because they are cost effective and stable even above 1000 °C.[2,9,18,19] Perovskite-type oxides usually display good activity for NO decomposition at high temperatures in the CRM.[3,18,19] For example, $Ba_{0.8}La_{0.2}Mn_{0.8}Mg_{0.2}O_3$, one of the most active perovskite-type oxides, displays catalytic activity for NO decomposition at temperatures up to 500 °C in the CRM.[19] However, the direct decomposition of NO over perovskite-type oxides is inhibited strongly by oxygen, which leads to a drastic decrease in NO conversion.[2,9] Thus, the direct catalytic decomposition of NO into N_2 and O_2 with high activity and N_2 selectivity at low temperature under excess oxygen is still a great challenge.

Recently, microwave-enhanced catalytic reactions have aroused tremendous attention as they show a drastic acceleration of the catalytic reaction rate and selectivity under mild conditions.[20–28] Furthermore, some chemical transformations that are impossible in the CRM can be performed successfully under the microwave reaction mode.[29–31] This significant microwave effect may provide a new route to address the following two main challenges for NO decomposition over perovskite-type oxides at a high reaction temperature with strong oxygen inhibition. There are several studies in which the microwave technique is applied to accelerate the reaction rate for NO removal by a microwave-discharge method[32–34] and microwave-assisted reduction method.[35–39] However, to date, little attention has been paid to the microwave direct catalytic decomposition of NO. Tang et al. reported direct NO decomposition over the Fe/ZSM-5 catalyst in the microwave-heating mode with 70% NO conversion.[40] Previously, our group reported the microwave direct decomposition of NO over physically mixed MeO_x-Cu-ZSM-5 (Me = Mn, Ni) catalysts[41] and $BaMn_{1-x}Mg_xO_3$ mixed oxides[42] at a low temperature under excess oxygen, in which the NO conversion reached 94.3% for MnO_2-Cu-ZSM-5 at 300 °C, 92.3% for Ni_2O_3-Cu-ZSM-5 at 350 °C, and 99.9% for $BaMn_{0.9}Mg_{0.1}O_3$ at 250 °C. Although the application of microwave irradiation to speed up chemical reactions continues to grow, the intrinsic nature of microwave irradiation on chemical reactions has still not been illuminated. In particu-

---

[a] W. Xu, Dr. J. Cai, Prof. J. Zhou, Y. Ou, W. Long, Z. You, Y. Luo
Key Laboratory of Green Catalysis and
Chemical Reaction Engineering of Hunan Province
School of Chemical Engineering
Xiangtan University
Xiangtan 411105 (P.R. China)
Fax: (+86) 731-58298173
E-mail: zhoujicheng@sohu.com

lar, there is still considerable controversy over the origin of the rate acceleration, whether it is caused by thermal microwave effects or nonthermal microwave effects.[21,22,29–31] Few investigations have focused on the decrease of the apparent activation energy under microwave irradiation.[43–45] We found that the activation energy for the direct catalytic decomposition of NO over MeO_x-Cu-ZSM-5 (Me = Mn, Ni) and $BaMn_{1-x}Mg_xO_3$ catalysts can be decreased significantly through microwave catalysis.[41,42]

The choice or development of outstanding catalysts for microwave catalytic reactions is of particular importance,[40,46,47] in view that catalysts selected or designed for their microwave-absorbing properties may speed up reactions drastically and even facilitate some chemical transformations that are impossible under the CRM.[47] However, no exact knowledge can provide a reference to select or develop a superb catalyst for microwave chemistry at the current stage.[40,46] Little attention has been paid to the direct decomposition of NO through microwave catalysis, particularly over perovskite-type oxides catalysts. Previously, we found that $BaMn_{1-x}Mg_xO_3$ mixed oxides have a good catalytic performance for the microwave direct decomposition of NO.[42] To the best of our knowledge, there are no reports on $BaMeO_3$ (Me = Mn, Co, Fe) mixed oxide catalysts for the direct decomposition of NO in the microwave catalytic reaction mode (MCRM), and the influence of Me sites on the microwave-absorbing properties and catalytic performance. Here, we report direct NO decomposition through microwave catalysis over $BaMeO_3$ (Me = Mn, Co, Fe) mixed oxides at low temperature under excess oxygen. The objective of this study is to evaluate the potential of the application of this new method as an effective NO_x emission control strategy and then to illustrate the influence of Me sites on the microwave-absorbing properties and catalytic performance under microwave irradiation.

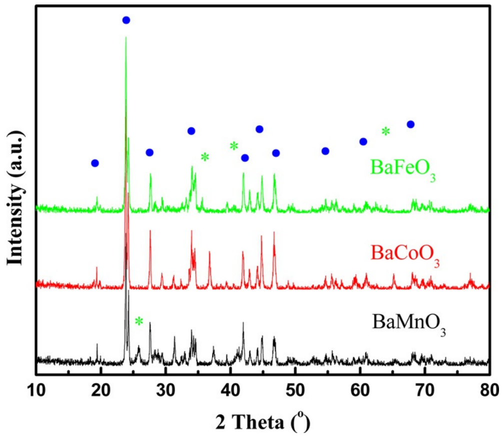

Figure 1. XRD patterns of $BaMnO_3$, $BaCoO_3$, and $BaFeO_3$ catalysts (● $BaCO_3$ and * $BaMeO_3$).

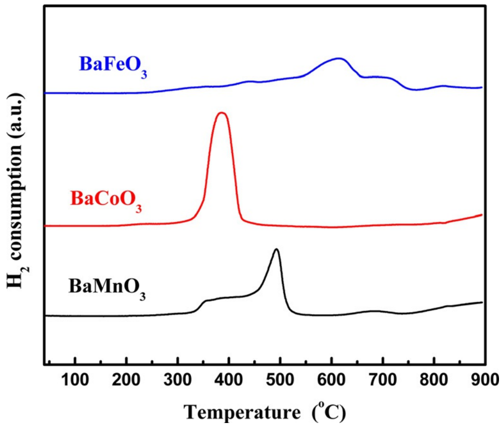

Figure 2. H_2-TPR profiles of $BaMnO_3$, $BaCoO_3$, and $BaFeO_3$ catalysts.

Results

Catalyst characterization

The XRD patterns of $BaMeO_3$ (Me = Mn, Co, Fe) are shown in Figure 1. All the $BaMeO_3$ (Me = Mn, Co, Fe) samples contain the diffraction peaks of the $BaMeO_3$ (Me = Mn, Co, Fe) phase, and the main diffraction peaks for all these samples can be assigned to the $BaCO_3$ phase, which indicates that $BaMeO_3$ (Me = Mn, Co, Fe) samples are mixed oxides. The thermal decomposition temperature of $BaCO_3$ is above 800 °C.[48] Therefore, $BaMeO_3$ (Me = Mn, Co, Fe) samples calcined at 700 °C in our present study generated mainly the $BaCO_3$ phase, which resembles the $La_{2-x}Ba_xNiO_4$ ($x = 0.6$–1.2) catalysts.[49]

H_2 temperature-programmed reduction (TPR) measurements were performed to investigate the relative reducibility of the $BaMeO_3$ (Me = Mn, Co, Fe) mixed oxides, and the results are listed in Figure 2. For the $BaMnO_3$ mixed oxide, only one main reduction peak at 493 °C and a shoulder peak at 355 °C can be observed. It has been reported extensively that the complete reduction of Mn^{4+}, Mn^{3+}, or Mn^{2+} into Mn^0 does not take place over Mn-based perovskite-type oxides.[50] However, this shoulder peak at 355 °C before the main reduction peak at 493 °C indicates the existence of Mn^{4+} in the structure of $BaMnO_3$, which is attributed to the reduction of Mn^{4+} into Mn^{3+} and finally into Mn^{2+}. For the $BaCoO_3$ mixed oxide, only one broad reduction peak between 377 and 395 °C can be observed. This phenomenon could be ascribed to the simultaneous reduction of Co^{4+} into Co^{3+} and Co^{3+} into Co^{2+}.[51] The temperature at the peak maximum (T_{max}) reflects the reducibility, and peak areas represent the total amount of H_2 consumed.[52] The T_{max} of $BaCoO_3$ of 387 °C is much lower than that of $BaMnO_3$ of 493 °C. Moreover, the total amount of H_2 consumed for $BaCoO_3$ is larger than that for $BaMnO_3$. For the $BaFeO_3$ mixed oxide, two reduction peaks at 616 and 693 °C can be observed. The former is associated with the reduction of Fe^{3+} into Fe^{2+}, and the latter is considered to be the reduction of Fe^{2+} into Fe^0.[51] The T_{max} of $BaMnO_3$ is much lower than that of $BaFeO_3$. Moreover, the total amount of H_2 consumed for $BaMnO_3$ is significantly larger than that for $BaFeO_3$. Therefore, these results suggest that the relative reducibility of these three samples increases in the order of $BaCoO_3 > BaMnO_3 > BaFeO_3$.

We also performed O_2 temperature-programmed desorption (TPD) experiments for $BaMeO_3$ (Me = Mn, Co, Fe), and the re-

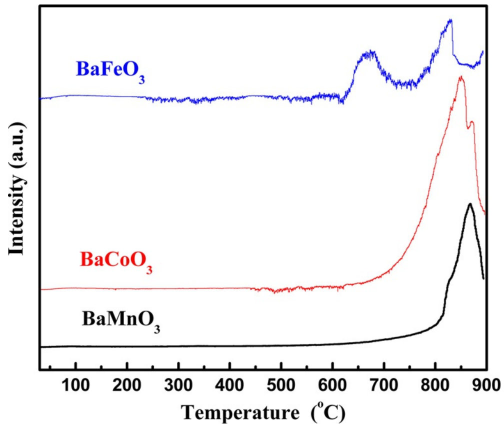

Figure 3. O_2-TPD profiles of $BaMnO_3$, $BaCoO_3$, and $BaFeO_3$ catalysts.

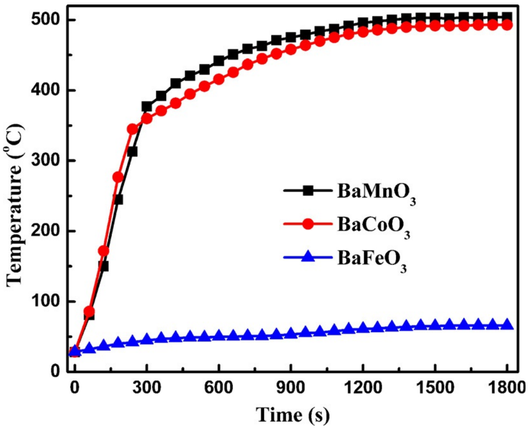

Figure 4. Microwave-heating behavior of $BaMnO_3$, $BaCoO_3$, and $BaFeO_3$ catalysts in the MCRM at a microwave power of 150 W.

sults are shown in Figure 3. Generally, there are three types of desorbed oxygen species over perovskite-type oxides.[49,52,53] The peak that appeared below 300 °C could be assigned to the desorption of ordinary chemically adsorbed and/or the weakest physically adsorbed molecular oxygen on the surface (denoted as α-O_2). The peak at 300–700 °C could be attributed to desorption of oxygen adsorbed chemically on oxygen vacancies (denoted as β-O_2). The peak at higher than 700 °C could be attributed to the lattice oxygen associated with the redox processes of Me ions (denoted as γ-O_2). Notably, $BaCO_3$ does not decompose to produce CO_2 below 900 °C.[48,54] Moreover, no O_2 desorption was observed for $BaCO_3$ in O_2-TPD previously.[55] Only one main desorption peak appeared for $BaMnO_3$, one main desorption peak with a small shoulder was seen for $BaCoO_3$ mixed oxide, and two desorption peaks for $BaFeO_3$ are apparent (Figure 3). The temperature of the desorption peak related to γ-O_2 is 869, 846, and 833 °C for $BaMnO_3$, $BaCoO_3$, and $BaFeO_3$, respectively. Moreover, a desorption peak related to β-O_2 is observed for the $BaFeO_3$ mixed oxide. The desorption temperature of $BaMnO_3$ and $BaCoO_3$ are much higher than that of $BaFeO_3$, even though the total amount of desorbed oxygen for $BaMnO_3$ and $BaCoO_3$ is larger than that of $BaFeO_3$. Therefore, the oxygen desorption capability increases in the order of $BaFeO_3 > BaCoO_3 > BaMnO_3$ (if we consider the desorption temperature and total amount of desorbed oxygen). However, the $BaMeO_3$ (Me = Mn, Co, Fe) mixed oxides reported here are not proper perovskite-type oxides according to the XRD results of $BaMeO_3$ (Me = Mn, Co, Fe; Figure 1).

Effects of reaction parameters under different reactor systems

Microwave-heating behavior of $BaMeO_3$ (Me = Mn, Co, Fe) catalysts in the MCRM

The desired temperature of the catalyst bed in the microwave catalytic reactor is highly dependent on the microwave-absorbing properties of the catalysts themselves. Here, the microwave-heating behavior of $BaMeO_3$ (Me = Mn, Co, Fe) was studied at a microwave power of 150 W in the MCRM. The catalyst-bed temperature increased with irradiation time, and a stable temperature was then maintained (Figure 4). The stable bed temperature was maintained at ~503 °C for $BaMnO_3$ and 493 °C for $BaCoO_3$ under microwave irradiation for ≈30 min at a microwave power of 150 W. In contrast, the stable temperature of the bed was maintained at only 66 °C for $BaFeO_3$ under the same microwave power and irradiation time. Clearly, the microwave-adsorbing ability of $BaMnO_3$ and $BaCoO_3$ is much better than that of $BaFeO_3$. The bed temperature of the $BaCoO_3$ sample is slightly higher than that of $BaMnO_3$ in the initial 5 min. Although the stable temperature of the $BaMnO_3$ sample is slightly higher than that of $BaCoO_3$, the microwave-adsorbing ability of these two catalysts is still almost similar. Therefore, $BaMnO_3$ and $BaCoO_3$ are excellent microwave-absorbing materials, whereas $BaFeO_3$ is a poor one. In the following experiments for the NO decomposition tests, the catalyst-bed temperature is maintained at a specific reaction temperature by regulating the microwave input power.

Effects of reaction temperature in the MCRM and CRM

The NO conversions as a function of reaction temperatures over $BaMeO_3$ (Me = Mn, Co, Fe) catalysts in the MCRM are shown in Figure 5. It is surprising that even at 100 °C (a very low reaction temperature for NO decomposition), the NO conversion is 43.2 % for $BaMnO_3$, 38.4 % for $BaCoO_3$, and 39.0 % for $BaFeO_3$ in the MCRM. The NO conversion over $BaMnO_3$ and $BaCoO_3$ catalysts increases initially and then decreases in the reaction temperature range of 100–400 °C. Importantly, the best NO conversion is up to 93.7 % for $BaMnO_3$ at 300 °C and 99.9 % for $BaCoO_3$ at 250 °C. Comparatively, Tang et al.[40] applied Fe/ZSM-5 as a catalyst for the direct decomposition of NO into N_2 and O_2 in the microwave-heating mode and achieved the highest NO conversion of only 70 %. To the best of our knowledge, except for our previous work,[42] there is no experimental study on the direct decomposition of NO with such a high NO conversion at such a low temperature under excess oxygen by microwave catalysis reported to date. Notably, the preparation route for $BaMn_xMg_{1-x}O_3$ catalysts in our previous

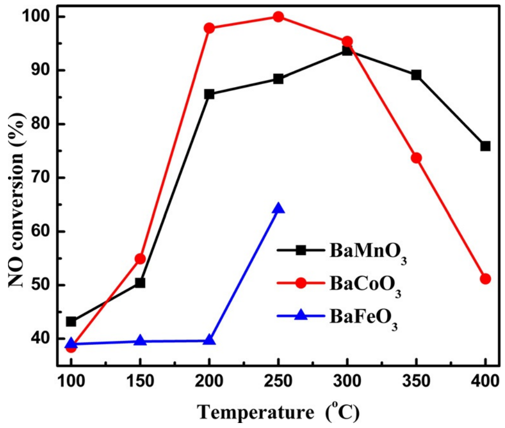

Figure 5. Effects of reaction temperature on NO conversion over $BaMnO_3$, $BaCoO_3$, and $BaFeO_3$ catalysts in the MCRM (reaction conditions: molar fraction of O_2, 5%; molar fraction of NO, 0.1%; $W/F = 1\ g\,s\,cm^{-3}$; and N_2 as the balance).

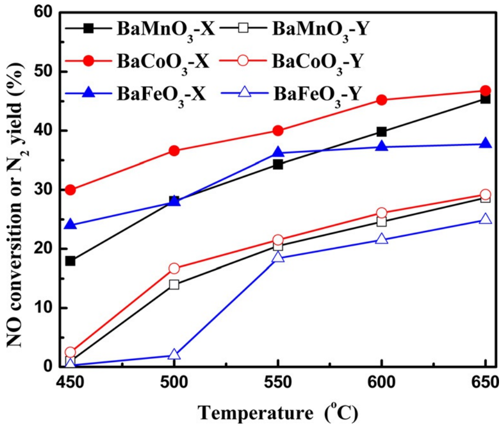

Figure 6. Effects of reaction temperature on NO conversion (*X*) and N_2 yield (*Y*) over $BaMnO_3$, $BaCoO_3$, and $BaFeO_3$ catalysts in the CRM (reaction conditions: molar fraction of O_2, 5%; molar fraction of NO, 0.1%; $W/F = 1\ g\,s\,cm^{-3}$; and N_2 as the balance).

work and $BaMnO_3$ mixed oxide in this work differs in the starting barium salts. However, the best NO conversion for $BaFeO_3$ is only 64.1% at 250 °C ($BaFeO_3$ is a poor microwave-absorbing material, which can be seen from Figure 4, and its catalyst-bed temperature can only increase to 250 °C in the MCRM at the maximum microwave power of 1000 W). Therefore, $BaMnO_3$ and $BaCoO_3$ catalysts display much a better catalytic performance for the microwave direct catalytic decomposition of NO than $BaFeO_3$. Clearly, $BaMnO_3$ and $BaCoO_3$ are outstanding microwave catalysts for the direct decomposition of NO, whereas $BaFeO_3$ is probably not suitable for this application. The catalytic performance of $BaCoO_3$ is better than that of $BaMnO_3$ as the reaction temperature was 150–300 °C. In particular, the best NO conversion of $BaCoO_3$ and $BaMnO_3$ is much higher than that of $BaFeO_3$. Therefore, the catalytic activity of $BaMeO_3$ (Me = Mn, Co, Fe) mixed oxides in the MCRM increases in the order of $BaCoO_3 > BaMnO_3 > BaFeO_3$.

To demonstrate microwave effects to speed up the direct decomposition of NO drastically, we also studied the catalyst performance of $BaMeO_3$ (Me = Mn, Co, Fe) in the CRM under identical conditions of reactor sizes, catalyst beds, reactant compositions, and total feed rate of the reactant gases, and the results are shown in Figure 6. Clearly, N_2 formation over these three catalysts starts at 450 °C, and the NO conversion at 450 °C is only 18.0, 30.0, and 24.0% for $BaMnO_3$, $BaCoO_3$, and $BaFeO_3$, respectively. The highest NO conversion and N_2 yield are, respectively, only 45.4% and 28.7% for $BaMnO_3$, 46.8% and 29.2% for $BaCoO_3$, and 37.7% and 24.9% for $BaFeO_3$ at 650 °C. Previous reports have shown that the $BaCO_3$ phase can play a crucial role to improve the activity of perovskite-type oxides for the direct decomposition of NO.[49,53] The $BaMnO_3$ mixed oxide in this study exhibits a slightly higher catalytic activity than the corresponding $BaMnO_3$ perovskite-type oxides in the literature,[19] probably because $BaMnO_3$ mixed oxide contains $BaCO_3$ as the main phase (Figure 1). However, $BaMnO_3$ and $BaCoO_3$ mixed oxides still show a surprisingly high catalytic activity at low temperatures in the MCRM (Figure 5). Clearly, the microwave catalytic effect improves the catalytic performance of $BaMnO_3$ and $BaCoO_3$ for the direct decomposition of NO drastically. Comparatively, the $BaFeO_3$ mixed oxide in the MCRM exhibits only a certain increase. Although the catalytic activity of $BaFeO_3$ at 550 °C is higher than that of $BaMnO_3$, $BaMnO_3$ still displays a higher catalytic performance than $BaFeO_3$ in the whole temperature range of 450–650 °C. Moreover, $BaMeO_3$ (Me = Mn, Co, Fe) mixed oxides in the CRM exhibit a similar catalytic activity for the direct decomposition of NO. Therefore, the catalytic performance of $BaMeO_3$ (Me = Mn, Co, Fe) mixed oxides in the CRM increases slightly in the order of $BaCoO_3 > BaMnO_3 > BaFeO_3$.

Effects of oxygen concentration in the MCRM and CRM

To further illustrate the impressively high catalytic performance of $BaMeO_3$ (Me = Mn, Co, Fe) mixed oxides, the direct decomposition of NO into N_2 and O_2 over $BaMeO_3$ (Me = Mn, Co, Fe) mixed oxides in the MCRM was performed in the presence of excess oxygen, and the results are shown in Figure 7. Surprisingly, the oxygen concentration does not influence NO conversion and N_2 selectivity in the MCRM. Importantly, the NO conversion and N_2 selectivity were up to 99.9% and 99.9%, respectively, for $BaCoO_3$ even with the coexistence of 10% oxygen. Moreover, the N_2 selectivity for $BaCoO_3$, $BaMnO_3$, and $BaFeO_3$ in the MCRM was more than 99.8, 94.4, and 92.4%, respectively. The high selectivity suggested that almost all of the NO transforms directly into N_2 and O_2, and undesired reactions between NO and O_2 to form NO_2 and the transformation of NO to N_2O hardly take place in the MCRM.

Normally, NO decomposition over perovskite-type oxides is inhibited strongly by the coexistence of oxygen. We also studied the effect of the oxygen concentration on the catalytic activity of $BaMeO_3$ (Me = Mn, Co, Fe) mixed oxides in the CRM under identical conditions, and the results are shown in Figure 7. Surprisingly, $BaMeO_3$ (Me = Mn, Co, Fe) mixed oxides in the CRM exhibit an extremely low catalytic activity in the absence of oxygen, and the NO conversion increases significantly with the oxygen concentration. This promoting effect of

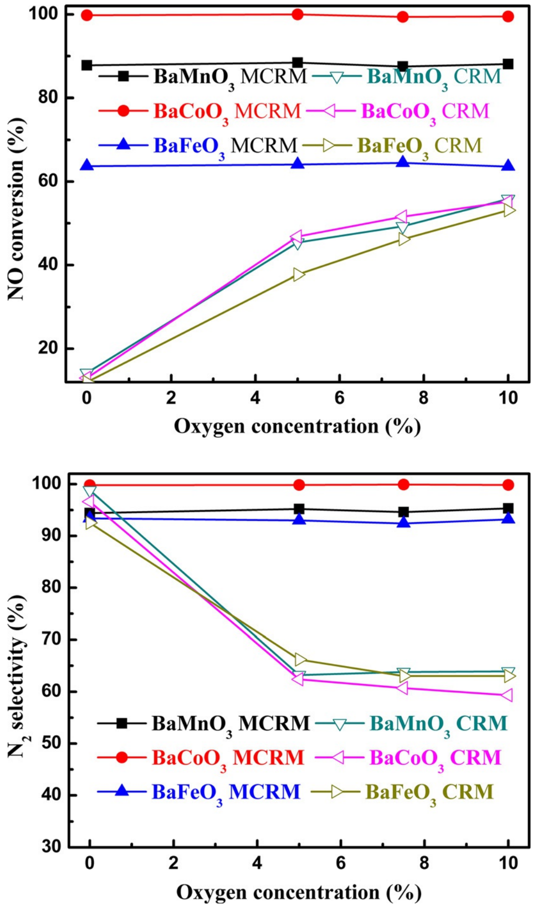

Figure 7. Effects of oxygen concentrations on a) NO conversion and b) N_2 selectivity over $BaMnO_3$, $BaCoO_3$, and $BaFeO_3$ catalysts in the MCRM and CRM (reaction conditions: reaction temperature, 250 °C in the MCRM and 650 °C in the CRM, respectively; molar fraction of NO, 0.1%; $W/F = 1\ g\,s\,cm^{-3}$; and N_2 as the balance).

oxygen on the NO decomposition was also reported in previous studies.[56–58] We speculate that the NO_2 generated during the reaction may be an intermediate species that plays an important role in the direct decomposition of NO.[49,56,58] In the presence of oxygen, the generation of NO_2 is favored. However, the surface of the catalyst is maintained in a highly oxidized state, which would be favorable for donor-type NO adsorption ($NO \rightarrow NO^+$), and the paring of nitrogen atoms could take place between NO^+ and NO_2.[56,58] Comparatively, almost no NO_2 was formed in the absence of oxygen, and hence the NO decomposition reaction hardly proceeds. At the same time, the appearance of the $BaCO_3$ phase, as the NO_2 storage component, is beneficial to improve the activity by adsorbing the intermediate NO_2 species, and thus $BaCO_3$ plays an important role to accelerate the catalytic recycling of NO decomposition.[49] In our cases, all three $BaMeO_3$ (Me = Mn, Co, Fe) mixed oxides contain the main phase of $BaCO_3$ deduced from the XRD results (Figure 1). The N_2 selectivity decreases sharply with the increase of oxygen concentration (Figure 7), which suggests an increase of the generation of NO_2. Therefore, the NO conversion increases with the oxygen concentration over $BaMeO_3$ (Me = Mn, Co, Fe) mixed oxides that contain the $BaCO_3$ phase in our case.

The oxygen concentration does not influence the catalytic performance of $BaMeO_3$ (Me = Mn, Co, Fe) mixed oxides in the decomposition of NO in the MCRM. This phenomenon is in accordance with our previous studies.[41,42] The microwave selective effect under microwave irradiation may account for this phenomenon. It is acknowledged widely that polar molecules can be activated by the microwave electromagnetic field.[20,47] As reported previously by us[39,41,42] and others,[32,38] NO molecules adsorbed on the active sites rather than O_2 molecules in the gas phase can be activated effectively by the microwave electromagnetic field. Although both O_2 and NO molecules can be adsorbed physically on the active sites, only NO molecules with a physical adsorption in the MCRM can be changed into chemical adsorption and further translate into N_2 and O_2. At the same time, O_2 molecules cannot be activated at such a low reaction temperature because of the microwave selective effect, and they are inactive to react with NO molecules to form NO_2. Therefore, $BaMeO_3$ (Me = Mn, Co, Fe) mixed oxides in the MCRM can still display an outstanding resistance to excess oxygen.

Effects of water vapor in the feed in the MCRM

It has been reported extensively that water vapor in the feed will inhibit the catalytic performance of perovskite-type oxide catalysts in the direct decomposition of NO in the CRM.[2,59] We investigated the effect of water vapor on NO conversion and N_2 selectivity over $BaCoO_3$ mixed oxide (one of the most active catalysts of the three mixed oxides in this study) in the MCRM. The NO conversion and N_2 selectivity display slight decreases in the presence of 5% H_2O (Figure 8). However, the $BaCoO_3$ mixed oxide catalyst still exhibits impressively high catalytic activity under wet conditions. Clearly, the $BaCoO_3$ mixed oxide catalyst in the MCRM displays a superior resistance to water vapor. Previously, we found that $BaMn_{0.9}Mg_{0.1}O_3$ displayed excellent resistance to water vapor in the MCRM.[42] In the CRM, the decreasing activity of a catalyst with the addition of H_2O is

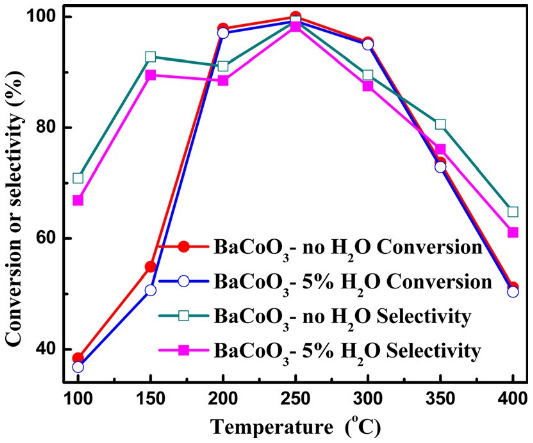

Figure 8. Effect of water vapor on the NO conversion over $BaCoO_3$ in the MCRM (reaction conditions: molar fraction of H_2O, 5%; molar fraction of O_2, 5%; molar fraction of NO, 0.1%; $W/F = 1\ g\,s\,cm^{-3}$; and N_2 as the balance).

because of the competitive adsorption of H_2O and NO molecules for the active sites.[2,38] However, H_2O is a strongly polar molecule and has a good microwave-absorbing ability. Therefore, H_2O molecules can interact with the catalyst in the microwave field as they are adsorbed on the catalyst, which results in a strong coupling and then the desorption of H_2O molecules from the adsorption sites, or weakening the adsorption of H_2O molecules on the catalytic surface.[38,40] Moreover, in the MCRM, it is possible to convert NO to the intermediate species of NO_2,[40] which plays an important role in the direct decomposition of NO.[49,56,58] Therefore, the $BaCoO_3$ catalyst in the MCRM can still display an outstanding catalytic performance in the presence of water.

Discussion

The above results indicate that the catalytic activity of $BaMeO_3$ (Me = Mn, Co, Fe) mixed oxides in the MCRM and CRM for the direct catalytic decomposition of NO increase in the order $BaCoO_3 > BaMnO_3 > BaFeO_3$. Moreover, the three $BaMeO_3$ (Me = Mn, Co, Fe) mixed oxides exhibit an extremely similar catalytic activity in the CRM, whereas they exhibit completely different catalytic performances in the MCRM. Importantly, $BaMnO_3$ and $BaCoO_3$ catalysts in the MCRM display a much better catalytic performance than $BaFeO_3$. Especially, the catalytic performance of $BaCoO_3$ in the MCRM is much better than that of $BaMnO_3$.

To analyze detailed factors that cause this different catalytic performance under these two different reactor systems, we first looked into some possible factors from the H_2-TPR and O_2-TPD results. The TPR results indicated that the relative reducibility increases in the order $BaCoO_3 > BaMnO_3 > BaFeO_3$. It is reported that the β- and γ-O_2 desorption peaks are interesting for the direct decomposition of NO and they are necessary to improve the activity of NO decomposition.[49,53] Clearly, the oxygen desorption ability seems to be the dominant parameter for the catalytic performance in the process of NO decomposition.[49,53] The catalytic activity of $BaMeO_3$ (Me = Mn, Co, Fe) mixed oxides in the CRM agrees well with the TPR and TPD results, and these three catalysts show a similar catalytic activity in the CRM. However, they have completely different catalytic performances in the MCRM. Therefore, the different catalytic performances in the MCRM and CRM cannot be explained simply by the TPR and TPD results.

We looked into some other possible factors from the microwave-absorbing properties. The microwave-heating behavior of these catalysts in the MCRM indicates that $BaMnO_3$ and $BaCoO_3$ have excellent microwave-absorbing properties, whereas that of $BaFeO_3$ is poor. The TPR and TPD results do not account for such completely different catalytic activities, in which $BaMnO_3$ and $BaCoO_3$ are more active than $BaFeO_3$ in the MCRM, whereas they are similar in the CRM. The only explanation of these results is probably from the differences in their microwave-absorbing properties. In the MCRM, different materials have different microwave-absorbing properties, which lead to a difference in the amount of microwave energy absorbed. Namely, the role of microwaves is not the same in the three catalysts. Comparatively, in the CRM, there is no difference. The stable bed temperatures of the $BaMnO_3$ and $BaCoO_3$ catalysts are much higher than that of $BaFeO_3$ (Figure 4). The ranking of catalytic performance is in accordance with the microwave-absorbing properties, and $BaMnO_3$ and $BaCoO_3$ display a much better performance than $BaFeO_3$ in the MCRM. Generally, a better microwave-absorbing catalyst can absorb more microwaves. Therefore, the microwave-absorbing properties may account for the completely different catalytic performance in the MCRM, even though the $BaMeO_3$ (Me = Mn, Co, Fe) mixed oxides exhibit very similar catalytic activities in the CRM.

At the same time, the microwave-adsorbing properties of $BaCoO_3$ and $BaMnO_3$ are similar. However, the $BaCoO_3$ catalyst displays a better catalytic performance than $BaMnO_3$ in the MCRM, and the best NO conversion of 99.9% for the $BaCoO_3$ catalyst is much higher than that of the $BaMnO_3$ catalyst of 93.7% in the MCRM. This different catalytic activity in the MCRM can be explained by the TPR and TPD results. The TPR and TPD results indicate that the reducibility and oxygen desorption capability of $BaCoO_3$ are better than those of $BaMnO_3$. Interestingly, the $BaCoO_3$ catalyst displays a slightly higher activity than $BaMnO_3$ in the CRM. However, the poor microwave-absorbing ability is the largest drawback for the $BaFeO_3$ catalyst. Therefore, $BaFeO_3$ shows the lowest activity compared with $BaCoO_3$ and $BaMnO_3$ in the MCRM.

To further elucidate the microwave catalytic effect on the decomposition of NO into N_2 and O_2, we computed the apparent activation energies (E_a') of these $BaMeO_3$ (Me = Mn, Co, Fe) catalysts for the decomposition reactions of NO. The calculated E_a' for $BaMnO_3$, $BaCoO_3$, and $BaFeO_3$ in the CRM is 194.5, 153.7, and 197.5 $kJ\,mol^{-1}$, respectively (Table 1). However, the corresponding E_a' values for $BaMnO_3$, $BaCoO_3$, and $BaFeO_3$ catalysts in the MCRM decrease to as low as 33.4, 13.7, and 46.7 $kJ\,mol^{-1}$, respectively. Similarly, Stiegman et al.[62] also found that the apparent activation energy decreased from 118.4 $kJ\,mol^{-1}$ under conventional convective heating to 38.5 $kJ\,mol^{-1}$ under microwave irradiation for the carbon–carbon dioxide (Boudouard) reaction. This high efficiency for the direct decomposition of NO into N_2 and O_2 over these catalysts in the MCRM at such a low temperature is mainly because of the significantly low E_a' values, which shows the excel-

Table 1. E_a' values for the direct catalytic decomposition of NO.

Mode/temperature conditions	Catalyst	E_a' [$kJ\,mol^{-1}$][a]	Reference
direct decomposition of NO	no catalyst	364	[60]
CRM, 579–733 K	Cu-ZSM-5	123	[16]
MCRM, 200–250 °C	$BaMnO_3$	33.4	this work
MCRM, 200–250 °C	$BaCoO_3$	13.7	this work
MCRM, 200–250 °C	$BaFeO_3$	46.7	this work
CRM, 600–650 °C	$BaMnO_3$	194.5	this work
CRM, 600–650 °C	$BaCoO_3$	153.7	this work
CRM, 600–650 °C	$BaFeO_3$	197.5	this work

[a] E_a' values were calculated by the Arrhenius equation; The first-order with respect to NO was used to calculate kinetic data.[61]

lent microwave catalytic effect of these materials under microwave irradiation.[41,42,44,45] Moreover, the E_a' value for $BaCoO_3$ is much lower than that of $BaMnO_3$ and $BaFeO_3$ in the MCRM. This is in accordance with the fact that $BaCoO_3$ has the best catalytic activity for the decomposition of NO in the MCRM. Importantly, the ranking of the catalytic performance of these three $BaMeO_3$ (Me = Mn, Co, Fe) catalysts in the MCRM is also in accordance with the E_a' values in the MCRM.

Most scientists today will agree that the energy of the microwave photon is too low to cleave molecular bonds directly.[29] However, the microwave electromagnetic field affects the target, which is not an intact chemical bond but the process of the destruction of old bonds or the formation of new bonds and potentially accelerates its passage through activation[63] as some chemical bonds could be weakened greatly in the process to form a new bond.[63] Interestingly, Kappe et al.[29] reported the direct interaction of the microwave electromagnetic field with specific molecules, intermediates, or even transition states in the reaction medium. Similarly, Wang et al.[38] reported that the direct interaction of a microwave electromagnetic field with a microwave-absorbing catalyst could cause a strong coupling in the catalyst, and also the coupling between the microwave electromagnetic field and NO_2 molecules may weaken the NO–O bond and promote its activation. The thermal effect of this reaction (direct catalytic decomposition of NO) can be neglected because N_2 and O_2 molecules absorb microwaves weakly and the NO concentration in the reactant gas is extremely low with a molar fraction of only 0.1%, which helps to illustrate the microwave catalytic effect in this reaction. Therefore, we can infer the fundamental mechanisms of decreasing apparent activation energies on the direct decomposition of NO under microwave irradiation as follows: First, the catalyst can be activated effectively by the microwave electromagnetic field through the absorption of microwave energy; second, NO rather than O_2 in the gas phase can be activated by the microwave electromagnetic field because microwaves can activate polar molecules.[32,38,39,41,42] The intrinsic reason for the decreasing activation energies under microwave irradiation is an interesting open issue, which requires further study. Further investigations are in progress in our laboratory to elucidate the nature of the microwave effect on heterogeneous catalytic reactions.

Conclusions

An attractive and environmental friendly process for NO_x emission control has been developed. Direct NO decomposition through microwave catalysis is impressively efficient in NO conversion and N_2 selectivity with values of up to 99.8% and 99.9%, respectively, for $BaCoO_3$ with 10% oxygen and a low temperature of 250 °C. Moreover, $BaCoO_3$ shows a superior resistance to water vapor. The best NO conversion is 93.7% for $BaMnO_3$ and only 64.1% for $BaFeO_3$. Synergistic effects between good microwave absorption, the best reducibility, and good oxygen desorption account for the best performance of $BaCoO_3$ in the microwave catalytic reaction mode. Importantly, the apparent activation energies of $BaMnO_3$, $BaCoO_3$, and $BaFeO_3$ decrease to as low as 33.4, 13.7, and 46.7 kJ mol^{-1}, respectively, which suggests a significant microwave catalytic effect. The whole catalytic activity in the microwave catalytic reaction mode is much higher than that in the CRM. Furthermore, microwave irradiation shows a microwave selective effect for these $BaMeO_3$ (Me = Mn, Co, Fe) catalysts, and the catalytic activity of NO decomposition under microwave irradiation is hardly influenced by the oxygen concentration.

Experimental Section

Preparation of catalysts

The $BaMeO_3$ (Me = Mn, Co, Fe) mixed oxides were prepared by a sol–gel method. Notably, the preparation of $BaMnO_3$ mixed oxide here and $BaMn_xMg_{1-x}O_3$ catalysts in our previous work is different in the barium salt, for which the barium salt used for the latter is $Ba(Ac)_2$.[42] In this work, $Ba(NO_3)_2$ (AR grade) and $Mn(NO_3)_2$ (AR grade) or $Co(NO_3)_2$ (AR grade) or $Fe(NO_3)_3$ (AR grade) were dissolved firstly in deionized water according to the stoichiometric amounts of $BaMeO_3$ (Me = Mn, Co, Fe) mixed oxides. Afterward, glycol and citric acid (the molar amounts of complexing species were 1.25 times of total metal cations) were added into the solutions. Subsequently, the solutions were stirred at 80 °C until amorphous gels were formed. The obtained gels were dried at 120 °C overnight, calcined in air at 400 °C for 2 h, and finally calcined at 700 °C for 4 h.

Catalyst characterization

Powder XRD patterns were recorded by using a Rigaku D/max-II/2500 X-ray powder diffractometer (CuK$_\alpha$ radiation).

H_2-TPR was conducted by using a FINESORB-3010 apparatus equipped with a thermal conductivity detector (TCD). Catalyst samples of 100 mg were placed in a quartz tube, purged under pure Ar with a flow of 10 mL min^{-1} at 200 °C for 30 min, and cooled to RT. The TPR profiles were recorded through passing a flow of 10% H_2 in Ar (10 mL min^{-1}) with heating from RT to 900 °C at a rate of 10 °C min^{-1}.

O_2-TPD was conducted by using a TP-5076 apparatus equipped with a TCD. Catalyst samples of 100 mg were placed in a quartz tube, purged under pure O_2 with a flow of 10 mL min^{-1} at 500 °C for 60 min, and cooled to RT. The TPD profiles were recorded through passing a flow of He (30 mL min^{-1}) with heating from RT to 900 °C at a rate of 10 °C min^{-1}.

Activity evaluation

Microwave reactor system

We designed a new microwave catalytic reactor system[41,42] to study the microwave effects in the gas–solid catalytic reactions. The experimental apparatus is presented in Figure 9. The reactor was composed of a microwave generator system and a catalytic reaction system. A 2.45 GHz microwave generator provided the microwave energy, and the microwave power was adjustable continuously in the range of 0–1000 W. The microwave magnetron source was connected to the resonant cavity by a rectangular waveguide. The catalytic activity tests were performed by using a quartz tube (540 mm in length and i.d.10 mm) at the center of resonant cavity. The reliable monitoring of reaction temperature is

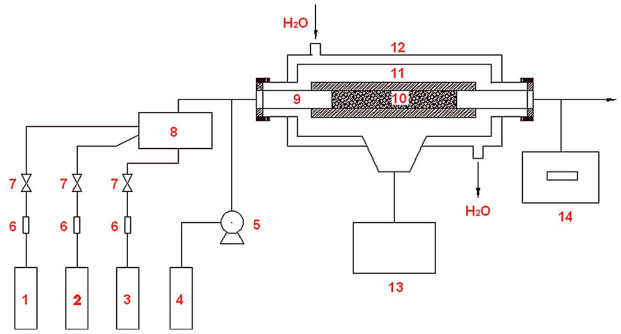

Figure 9. Schematic diagram of the microwave catalytic reactor system. 1. NO; 2. O_2; 3. N_2; 4. Storage tank; 5. Metering pump; 6. Mass-flow meter; 7. Valve; 8. Premixer; 9. Quartz reactor; 10. Fixed bed; 11. Thermal insulation; 12. Resonant cavity; 13. Microwave generator; 14. On-line NO_x analyzer.

nontrivial but absolutely critical to the investigation of microwave effects.[43] Therefore, a thermocouple probe inserted into the catalyst bed was used to measure the catalyst-bed temperature precisely.

Catalytic activity tests

The catalyst bed contained 2 g of the catalyst (40–60 mesh). The reactant gas mixtures consisted of 0.1 vol% NO, 0–10.0 vol% O_2, and N_2 as the balance gas. The total feed rate of the reactant gases were fixed at $W/F = 1\ \mathrm{g\,s\,cm^{-3}}$, in which W and F are the catalyst weight and the total flow rate of reactant mixtures, respectively. For comparison, the MCRM and CRM were performed under the same reaction conditions of reactor sizes, catalyst beds, reactant compositions, and total feed rate of the reactant gases. A microreactor device (MRT-6123; Beijing Xin Hang Shield Petrochemical Technology Co., Ltd.) was used to perform the catalytic activity tests in the CRM. All the activity values were measured at each temperature under steady-state conditions. An online NO_x analyzer (42C, Thermo Environmental Instruments Co., Ltd., U.S.) was used to measure the concentrations of NO and NO_2 in the products. Besides, the analysis system also has GC (Agilent 7890A TCD) with a Poropak Q column for the analysis of N_2O. In the MCRM and CRM, the main product was N_2, the byproduct was NO_2, and N_2O was not detected. Therefore, we can compute the NO conversion (X(NO)), N_2 selectivity ($S(N_2)$), and N_2 yield ($Y(N_2)$) according to the conservation of nitrogen by Equations (1)–(3) as follows:

$$X(NO) = \frac{C_0(NO) - C_1(NO)}{C_0(NO)} \times 100\% \tag{1}$$

$$S(N_2) = \frac{C_0(NO) - C_1(NO) - C_1(NO_2)}{C_0(NO) - C_1(NO)} \times 100\% \tag{2}$$

$$Y(N_2) = X(NO) \times S(NO) = \frac{C_0(NO) - C_1(NO) - C_1(NO_2)}{C_0(NO)} \times 100\% \tag{3}$$

in which C_0(NO) represents the NO concentration before the reaction and C_1(NO) and $C_1(NO_2)$ represent the NO and NO_2 concentration after the reaction, respectively.

Acknowledgements

We greatly appreciate financial support from the National Natural Science Foundation of China (No.20976147, 21506184), Science and Technology Foundation of Hunan Province, China (No.2014K4048), China Postdoctoral Science Foundation (No.2015M572258), and PhD Startup Foundation of Xiangtan University (No.15QDZ13). We also sincerely appreciate the support by Synotherm Corporation for microwave experimental apparatus.

Keywords: barium · cobalt · manganese · microwave chemistry · nitrogen oxides

[1] J. N. Galloway, A. R. Townsend, J. W. Erisman, M. Bekunda, Z. C. Cai, J. R. Freney, L. A. Martinelli, S. P. Seitzinger, M. A. Sutton, *Science* **2008**, *320*, 889 – 892.
[2] N. Imanaka, T. Masui, *Appl. Catal. A* **2012**, *431*, 1 – 8.
[3] H. Q. Jiang, L. Xing, O. Czuprat, H. Wang, S. Schirrmeister, T. Schiestel, J. Caro, *Chem. Commun.* **2009**, 6738 – 6740.
[4] J. Zhu, Y. Wei, W. Chen, Z. Zhao, A. Thomas, *Chem. Commun.* **2010**, *46*, 6965 – 6967.
[5] A. Amirnazmi, J. E. Benson, M. Boudart, *J. Catal.* **1973**, *30*, 55 – 65.
[6] J. M. D. Cónsul, C. A. Peralta, E. V. Benvenutti, J. A. C. Ruiz, H. O. Pastore, I. M. Baibich, *J. Mol. Catal. A* **2006**, *246*, 33 – 38.
[7] M. Haneda, Y. Kintaichi, I. Nakamura, T. Fujitani, H. Hamada, *Chem. Commun.* **2002**, 2816 – 2817.
[8] E. R. S. Winter, *J. Catal.* **1971**, *22*, 158 – 170.
[9] N. Imanaka, T. Masui, H. Masaki, *Adv. Mater.* **2007**, *19*, 3660 – 3663.
[10] J. J. Yu, X. P. Wang, L. D. Li, Z. P. Hao, Z. P. Xu, G. Q. Lu, *Adv. Funct. Mater.* **2007**, *17*, 3598 – 3606.
[11] W. J. Hong, S. Iwamoto, S. Hosokawa, K. Wada, H. Kanai, M. Inoue, *J. Catal.* **2011**, *277*, 208 – 216.
[12] M. Haneda, Y. Kintaichi, N. Bion, H. Hamada, *Appl. Catal. B* **2003**, *46*, 473 – 482.
[13] M. Iwamoto, H. Furukawa, Y. Mine, F. Uemura, S. I. Mikuriya, S. Kagawa, *J. Chem. Soc. Chem. Commun.* **1986**, 1272 – 1273.
[14] M. Y. Kustova, S. B. Rasmussen, A. L. Kustov, C. H. Christensen, *Appl. Catal. B* **2006**, *67*, 60 – 67.
[15] C. Yun, G. M. Jon, *J. Catal.* **1998**, 178, 408 – 413.
[16] V. Tomašić, Z. Gomzi, S. Zrnčević, *Appl. Catal. B* **1998**, *18*, 233 – 240.
[17] V. I. Pârvulescu, M. A. Centeno, P. Grange, B. Delmon, *J. Catal.* **2000**, *191*, 445 – 455.
[18] J. Zhu, A. Thomas, *Appl. Catal. B* **2009**, *92*, 225 – 233.
[19] H. Iwakuni, Y. Shinmyou, H. Yano, H. Matsumoto, T. Ishihara, *Appl. Catal. B* **2007**, *74*, 299 – 306.
[20] W. C. Conner, G. A. Tompsett, *J. Phys. Chem. B* **2008**, *112*, 2110 – 2118.
[21] X. Zhang, D. Hayward, *Inorg. Chim. Acta* **2006**, *359*, 3421 – 3433.
[22] X. L. Zhang, D. O. Hayward, D. M. P. Mingos, *Chem. Commun.* **1999**, 975 – 976.
[23] M. Larhed, C. Moberg, A. Hallberg, *Acc. Chem. Res.* **2002**, *35*, 717 – 727.
[24] S. Gopalakrishnan, J. Munch, R. Herrmann, W. Schwieger, *Chem. Eng. J.* **2006**, *120*, 99 – 105.
[25] A. B. A. A. Nassr, M. Bron, *ChemCatChem* **2013**, *5*, 1472 – 1480.
[26] M. T. Radoiu, Y. Chen, M. C. Depew, *Appl. Catal. B* **2003**, *43*, 187 – 193.
[27] B. Fidalgo, A. Arenillas, J. A. Menéndez, *Appl. Catal. A* **2010**, *390*, 78 – 83.
[28] X. R. Zhang, L. C. Wang, Y. Cao, W. L. Dai, H. Y. He, K. N. Fan, *Chem. Commun.* **2005**, 4104 – 4106.
[29] C. O. Kappe, B. Pieber, D. Dallinger, *Angew. Chem. Int. Ed.* **2013**, *52*, 1088 – 1094; *Angew. Chem.* **2013**, *125*, 1124 – 1130.
[30] D. Obermayer, B. Gutmann, C. O. Kappe, *Angew. Chem. Int. Ed.* **2009**, *48*, 8321 – 8324; *Angew. Chem.* **2009**, *121*, 8471 – 8474.
[31] G. Shore, S. Morin, M. G. Organ, *Angew. Chem. Int. Ed.* **2006**, *45*, 2761 – 2766; *Angew. Chem.* **2006**, *118*, 2827 – 2832.
[32] J. W. Tang, T. Zhang, D. B. Liang, C. H. Xu, X. Y. Sun, L. W. Lin, *Chem. Commun.* **2000**, 1861 – 1862.
[33] J. Tang, T. Zhang, Z. Ma, N. Li, *Ind. Eng. Chem. Res.* **2003**, *42*, 5993 – 5999.

[34] Y. Chang, A. Sanjurjo, J. G. McCarty, G. Krishnan, B. Woods, E. Wachsman, *Catal. Lett.* **1999**, *57*, 187 – 191.
[35] Z. S. Wei, G. H. Zeng, Z. R. Xie, *Energy Fuels* **2009**, *23*, 2947 – 2951.
[36] C. Y. Cha, D. S. Kim, *Carbon* **2001**, *39*, 1159 – 1166.
[37] J. W. Tang, T. Zhang, L. Ma, N. Li, D. B. Liang, L. W. Lin, *J. Catal.* **2002**, *211*, 560 – 564.
[38] X. D. Wang, T. Zhang, C. H. Xu, X. Y. Sun, D. B. Liang, L. W. Lin, *Chem. Commun.* **2000**, 279 – 280.
[39] W. T. Xu, J. C. Zhou, H. Li, P. F. Yang, Z. M. You, Y. S. Luo, *Fuel Process. Technol.* **2014**, *127*, 1 – 6.
[40] J. W. Tang, T. Zhang, D. Liang, H. Yang, N. Li, L. W. Lin, *Appl. Catal. B* **2002**, *36*, 1 – 7.
[41] W. Xu, J. Zhou, Z. You, Y. Luo, Y. Ou, *ChemCatChem* **2015**, *7*, 450 – 458.
[42] W. Xu, J. Zhou, Y. Ou, Y. Luo, Z. You, *Chem. Commun.* **2015**, *51*, 4073 – 4076.
[43] B. Temur Ergan, M. Bayramoglu, *Ind. Eng. Chem. Res.* **2011**, *50*, 6629 – 6637.
[44] J. S. K. Kim, S. Dong, *Fuel Sci. Technol. Int.* **1993**, *11*, 1175 – 1183.
[45] Y. Kong, C. Y. Cha, *Carbon* **1996**, *34*, 1035 – 1040.
[46] X. Wang, L. Mei, X. Xing, L. Liao, G. Lv, Z. Li, L. Wu, *Appl. Catal. B* **2014**, *160*, 211 – 216.
[47] M. Crosswhite, J. Hunt, T. Southworth, K. Serniak, A. Ferrari, A. E. Stiegman, *ACS Catal.* **2013**, *3*, 1318 – 1323.
[48] I. Arvanitidis, D. Siche, S. Seetharaman, *Metall. Mater. Trans. B* **1996**, *27*, 409 – 416.
[49] Y. Zhu, D. Wang, F. Yuan, G. Zhang, H. Fu, *Appl. Catal. B* **2008**, *82*, 255 – 263.
[50] S. Royer, H. Alamdari, D. Duprez, S. Kaliaguine, *Appl. Catal. B* **2005**, *58*, 273 – 288.
[51] B. Levasseur, S. Kaliaguine, *Appl. Catal. A* **2008**, *343*, 29 – 38.
[52] J. Zhu, H. Li, L. Zhong, P. Xiao, X. Xu, X. Yang, Z. Zhao, J. Li, *ACS Catal.* **2014**, *4*, 2917 – 2940.
[53] J. Zhu, D. Xiao, J. Li, X. Yang, *Catal. Lett.* **2009**, *129*, 240 – 246.
[54] L. A. Al-Hajji, M. A. Hasan, M. I. Zaki, *J. Therm. Anal. Calorim.* **2010**, *100*, 43 – 49.
[55] C. T. Au, H. He, S. Y. Lai, C. F. Ng, *J. Catal.* **1996**, *163*, 399 – 408.
[56] Z. Liu, J. Hao, L. Fu, T. Zhu, *Appl. Catal. B* **2003**, *44*, 355 – 370.
[57] K. Tabata, *J. Mater. Sci. Lett.* **1988**, *7*, 147 – 148.
[58] F. Buciuman, E. Joubert, J. Menezo, J. Barbier, *Appl. Catal. B* **2001**, *35*, 149 – 156.
[59] C. Tofan, D. Klvana, J. Kirchnerova, *Appl. Catal. B* **2002**, *36*, 311 – 323.
[60] S. Roy, M. S. Hegde, G. Madras, *Appl. Energy* **2009**, *86*, 2283 – 2297.
[61] Y. Teraoka, T. Harada, S. Kagawa, *J. Chem. Soc. Faraday Trans.* **1998**, *94*, 1887 – 1891.
[62] J. Hunt, A. Ferrari, A. Lita, M. Crosswhite, B. Ashley, A. E. Stiegman, *J. Phys. Chem. C* **2013**, *117*, 26871 – 26880.
[63] K. Huang, X. Yang, *Prog. Nat. Sci.* **2006**, *16*, 273 – 279.

Received: August 30, 2015
Revised: September 17, 2015